

Article

Self-Assembly of Self-Cleaning Polystyrene/Styrene-Butadiene-Styrene Films with Well-Ordered Micro-Structures

Yang Liu, Jianchao Deng, Yamei Wang, Xiaoyang Zhan, Deyuan Zhang and Huawei Chen *

School of Mechanical Engineering and Automation, Beihang University, Beijing 100191, China; liuyang168@buaa.edu.cn (Y.L.); dengj_c@163.com (J.D.); wangym93@buaa.edu.cn (Y.W.); ZY2007429@buaa.edu.cn (X.Z.); zdybuaa@163.com (D.Z.)

* Correspondence: chenhw75@buaa.edu.cn; Tel.: +86-010-8233-9717

Received: 18 October 2020; Accepted: 21 November 2020; Published: 22 November 2020



Abstract: Well-ordered porous films have been widely applied in various areas, such as chemical sensors, microreactors, and tissue engineering. In this article, we propose a novel air-liquid interface self-assembly method to fabricate well-ordered porous polystyrene (PS)/styrene-butadiene-styrene (SBS) films by simply dipping the PS/SBS chloroform solutions onto the surface of a mixed water/ethanol liquid phase. The proper volume ratio of water/ethanol is necessary for the formation of films with highly uniform pore size. The effect of weight ratio of PS/SBS, the volume ratio of water/ethanol and the concentration of the solutions were experimentally investigated. The pore size decreases with the concentration of polymer solution, and the structure becomes more regular with the decrease of water/ethanol volume ratio. Ordered structure can be formed under PS/SBS in a certain weight ratio. The self-assembled films also have the function of self-cleaning. Besides the analysis of structural characteristic, the self-assembly mechanism was also discussed.

Keywords: self-assembly; interface; films; porous materials; self-cleaning

1. Introduction

Well-ordered porous films have potential applications in optoelectronic devices on a large scale [1], filtration membranes [2,3], tissue engineering [4,5], super-hydrophobic surface [6,7], catalysis [8,9] and so on. A variety of top-down methods, such as standard microelectronic fabrication process (e.g., plasma etching, photolithography) and soft lithography have been applied to fabricate well-ordered porous films [10]. However, these methods have a number of disadvantages, such as high-cost, time-consuming, and complicated fabricating processes. Compared with the abovementioned top-down approaches, self-assembly approaches, including microphase separation [11,12], sol-gel [13,14], templating [15] and nanoparticle assembly [16,17], are simple and effective. In these a basic structure unit (molecule, nanometer material, micrometer material or in a larger scale) spontaneously forms an ordered structure [18].

The air-liquid interface is the traditional medium to fabricate molecular assemblies such as Langmuir-Blodgett films, and ultrathin films of materials [8]. Monolayers, nanowire arrays, long-range well-ordered nanostructure and 2-dimensional Ag nanoparticle films have been fabricated by this method [19–23]. The surface features obtained by self-assembly at the air-liquid interface are connected with the nature and relative lengths of the blocks, concentration of the spreading solution, pH, surface pressure, etc. [24,25]. Amphiphilic polymers (block copolymers, π -conjugated polymers, etc.), dendrimers (poly(benzyl ether), poly(amido amine), etc.) and metal nanoparticles have all been studied in the air-liquid interface self-assembly method [26]. The behavior of hydrophobic conjugated

block copolymers' self-assembly at the air-liquid interface has been studied and the direct structural evidence has been provided [27,28]. However, the films fabricated by this method are usually ultrathin and their adhesion to the desired substrate is weak and the morphology is not well-ordered either. Moreover, the procedure is complex and usually needs an isobaric environment. In addition, water is always used as the liquid in this experiment, which might restrict other experimental implications of this method. In our opinion, porous films with regular patterns made from pure polymers have not yet been fabricated at the air-liquid interface through self-assembly [27].

In this article, we develop an effective one-step strategy to synthesize well-ordered porous films by dissolving PS and SBS in chloroform, and then dipping the solution in a water/ethanol liquid mixture. The solutions could self-assemble into the desired films at the interface of air and the mixed liquid. The morphologies of films could be tuned by varying the weight ratio of PS/SBS in chloroform, as well as by varying the volume ratio of water/ethanol and the concentration of the PS/SBS chloroform solutions. This method could be applied to numerous devices to fabricate microstructure films. Furthermore, after treatment with a lubricant, the films can display excellent self-cleaning ability.

2. Experimental

2.1. Materials

PS ($M_w = 150,000$) and SBS (KTR-101, $80,000 \leq M_w \leq 120,000$, 30 wt % PS) were purchased from Sigma-Aldrich (Shanghai) Trading Company Limited (Shanghai, China) and Kumho Petrochemical (Seoul, Korea), respectively. Ethanol (G.R.) and chloroform (A.R.) were purchased from Beijing Chemical Works (Beijing, China). The perfluoropolyether lubricant (DuPont Krytox GPL100, surface tension $17 \text{ m}\cdot\text{Nm}^{-1}$), viscosity $0.124 \text{ cm}^2 \text{ s}^{-1}$ at $20 \text{ }^\circ\text{C}$) was purchased from DuPont Corporation (Wilmington, DE, USA). All chemicals were used as received. The water used throughout the experiments was deionized water. The blood used in the experiments came from laboratory mice.

2.2. Porous Films Formation

The solutions were prepared in the beaker by dissolving the mixture of PS and SBS at different weight ratio in chloroform. The solutions were well sealed and left undisturbed for 48 h at ambient temperature in the dark to ensure the mixture dissolved completely and the decelerate evaporation of the solvent, and the dipping experiment should be finished within next 7 days. A few drops (0.1–0.3 mL) of the as-made solutions with varied concentrations were dipped onto the surface of the mixed water/ethanol liquid with different volume ratios in a glass petri dish. After several minutes of incubation, the ivory-white films would form at the air-liquid interface. The films were then transferred to a glass substrate and porous films were obtained. The glass substrates used for depositing films were ultra-sonicated separately in hexane, acetone, and ethanol for 15 min, and then put it in a vacuum environment $50 \text{ }^\circ\text{C}$ for 30 min.

2.3. Sample Characterization

Surface morphologies of porous films were characterized by using a scanning electron microscope (SEM, SU8000, Hitachi, Tokyo, Japan), operating at a 10 kV accelerating voltage. The samples were sputtered with gold, the thickness of which was about 20 nm. On basis of SEM images, the pore size and distribution were analyzed by Image-pro Plus software (Media Cybernetics, Bethesda, MD, USA).

3. Results and Discussion

3.1. Formation Mechanism

The properties of the liquid are essential to the features of the films, and ethanol plays a critical role in the formation of well-ordered porous films. The formation of porous films could be explained as follows: on the one hand, ethanol reduces the surface tension of the water, so the PS/SBS solution

would stay on the liquid surface instead of spreading over the liquid surface immediately (Figure 1A). The PS block will gather together as the chloroform evaporation occurs (Figure 1B). On the other hand, ethanol's high evaporation rate would speed up the evaporation of the chloroform. With chloroform's further evaporation, the PS-water interactions would result in the hole's formation just as Matthew et al. have explained (Figure 1C) [29]. There are mainly three intermolecular forces between the particles in solution: van der Waals force, hydrophobic force and hydrogen-bonding force in the self-assembly system. Except these three forces, the surface tension of air-liquid also exists in this case. The repulsion of PS block and the PS phase of SBS take the priority in the assembly process (Figure 1D). To maintain the balance of the system, the structure would compromise between complete disorder and perfect order. The most stable structure would be an array of hexagons of equal size. However, due to entropic effects, such a situation is never reached [30]. In our case, the ordered porous poles finally formed (Figure 1E) at the end of the assembly process. As for SBS, which contains the PS hard phase and the PB soft phase [31], we anticipate the function of PB block is to assist the well-form of the films, which will be discussed in the next part. Furthermore, when the polymer solution dropped on the mixed liquid dropwise and continuously, the polymer solution drop would accumulate and form a film on a large scale which could be attached to the free-form surface (Figure 1F).

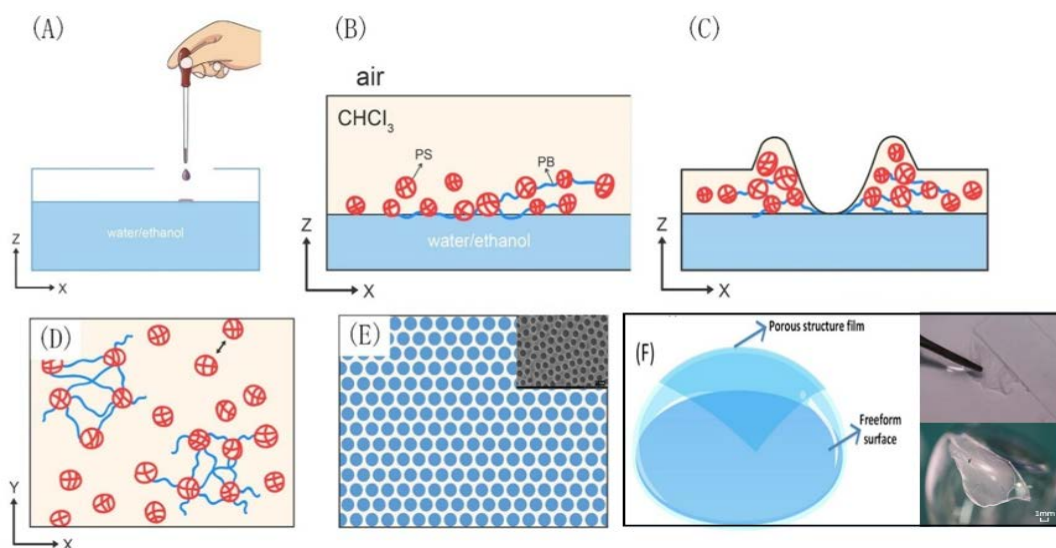


Figure 1. Schematic of PS/SBS films formation at the air-liquid interface. (A) Drop the PS/SBS chloroform polymer solution on the surface of the mixed liquid of water and absolute ethanol. (B) PS gathered on the liquid phase slowly. (C) As the chloroform evaporates and anhydrous ethanol can accelerate its evaporation rate, the PS further accumulates and finally collapses to form pores. (D) Schematic diagram of PS gathering on the horizontal plane. (E) Schematic diagram of the porous structure of the resulting membrane. (F) Schematic diagram of application that can be applied on curved surface: left: Schematic diagram, right: The prepared film can completely fall off the substrate (glass surface) and fit well on curved surfaces.

3.2. Influence of Volume Ratio of the Water/Ethanol

The air-liquid interfacial self-assembly method is usually carried out at the air-water interface. However, as shown in Figure 1, there are some microstructures appeared when the PS/SBS films self-assembled (the concentration of the solution is 50 g/L and the weight ratio of PS/SBS is 3:1) at the air-water interface namely the structure is disordered. After introduction of the ethanol, the films were formed and the structure was well-ordered. To get a better understanding of the ethanol's function in this system, several controlled experiments were implemented. Mixed water/ethanol liquid with different volume ratios (1:0, 10:1, 8:1, 6:1, 4:1, 3:1, 2:1) were prepared. When the volume ratio of water/ethanol is less than 2:1, no matter what the weight ratio of PS/SBS and the concentration of the

spreading solution are, no films were observed. The solution would settle and produced white floccus in the mixed liquid as the ethanol concentration is increased. As shown in Figure 2, when the weight ratio of PS/SBS is 3:1 and the concentration of the solution is 70 g/L, the structure of the films is more well-ordered. There is no big difference in morphology when the volume ratio of water/ethanol is 6:1 and 4:1 (Figure 2D,E). However, when the volume ratio of water/ethanol is 2:1, the morphology (Figure 2G) changes sharply, both micro- and macroscopically. Macroscopically, the diameter of the films is usually 5~15 mm (the large ordered structure of the film, see Figure S1) except when the volume ratio of water/ethanol is 2:1, when the latter is about 1 mm. Microscopically, the diameter of the pole is smaller than the formers' and has a unique "peristome" (Figure 2H) which never exists in the others. When the volume ratio of water/ethanol is 2:1, the "peristome" also exists in other concentrations of the solution and different weight ratio of PS/SBS (Figure S2). The average pore diameter increases with the decrease of the water/ethanol's volume ratio when it is between 10:1 and 3:1 (Figure 3), as well as the pore pitch. But when the volume ratio of water/ethanol is 2:1, the average pore diameter decreased to 4.35 μm .

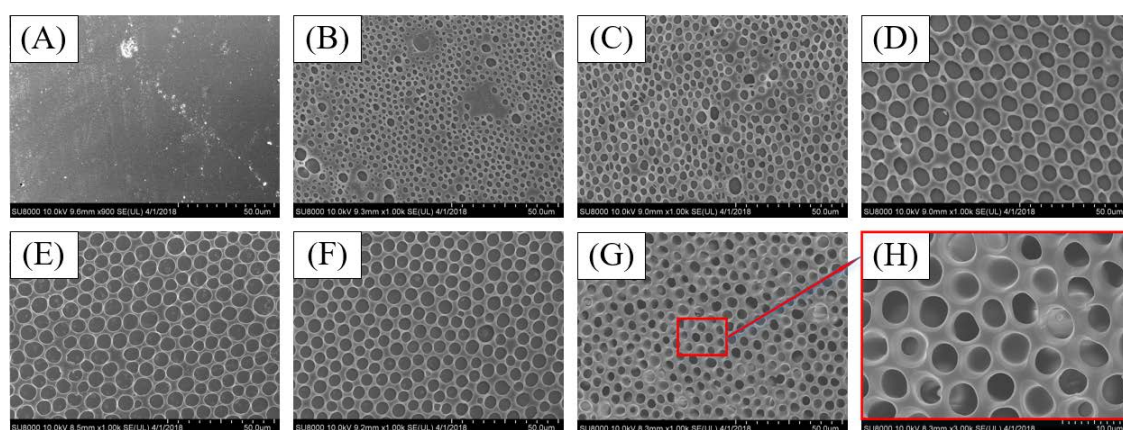


Figure 2. SEM images of PS/SBS porous films formed at different volume ratios of water/ethanol. (A) 1:0, (B) 10:1, (C) 8:1, (D) 6:1, (E) 4:1, (F) 3:1, (G) 2:1, (H) 2:1. Other factors: concentration 70 g/L, weight ratio of PS/SBS 3:1.

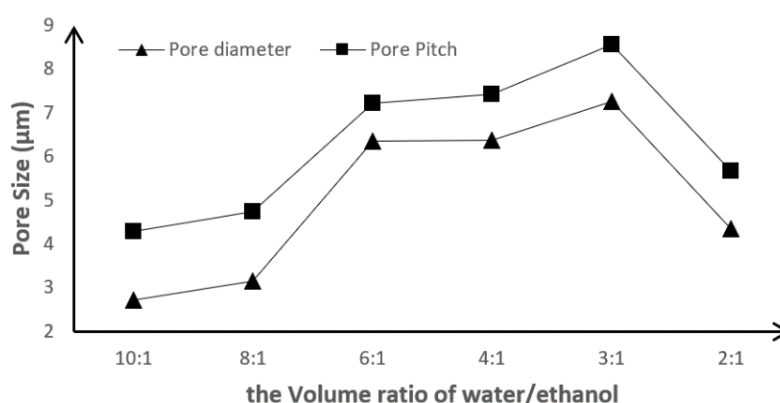


Figure 3. Plots of pore size versus the volume ratio of water/ethanol.

With the increase of ethanol, the surface tension of the mixed liquid decreases, so the PS/SBS solution would not spread over the water surface rapidly and forms an ultrathin film. The reducing surface tension of the mixed liquid assists in the formation of the poles. Meanwhile, the PS/SBS solutions would be suitable to self-assemble at a substrate surface with lower surface tension. When the volume ratio of water/ethanol was 2:1, the chloroform would evaporate more quickly with the assistance of ethanol, so the "peristome" appeared. The "peristome" also appeared at other concentrations and

different weight ratio of PS/SBS, but the volume ratio of the water/ethanol was still 2:1 (Figure S2). The surface tension of the mixed liquid was too low when the volume ratio is less than 2:1, so the liquid surface could not support the PS/SBS solution. It is worth mentioning that if the volume of the PS/SBS solution is greater than 0.4 mL, it would form an ellipsoid and sink into the mixed liquid, after the turbulence (use the dropper to stick the solution), the solution would break up into small ones and float on the liquid's surface, while the films will form again.

We also observed that some wrinkles appear at the edge of the films when the weight ratio of PS/SBS is greater than 4:1. Generally, wrinkle formation has been understood as a relaxation process of redundant stress accumulated in a bilayer system containing a hard thin film top layer and a soft substrate layer. When the bilayer system is under in-plane compressive stress which exceeds a critical compression, the hard skin thin film top layer will relax the excessive stresses by out-of-plane deformation [32]. When the collective repulsion between the PS exceeds the compression of the blended films, the wrinkles appeared.

3.3. Influence of Weight Ratio of the PS/SBS

The weight ratio of PS/SBS exerts an enormous impact on porous films formation. In order to investigate the influence of weight ratio on the PS/SBS, we prepared the PS/SBS chloroform solutions with different weight ratio (1:0, 10:1, 8:1, 5:1, 4:1, 3:1, 2:1, 1:1, 1:2, 1:3, 1:4, 1:6, 1:8, 1:10, 0:1) of PS/SBS, the concentration of the solutions is 50 g/L and the volume ratio of the water/ethanol is 3:1. As shown in Figure 4, in the PS/SBS blending system, with a little addition of SBS (Figure 4B), the structures are disordered compared to the no-SBS system (Figure 4A) but they become more regular, and also the pore size is reducing with the further addition of the SBS (Figure 4C–F). However, when the weight ratio of PS/SBS is less than 3:1, the structures become disordered again with the increase of the SBS (Figure S3A–C); when the ratio is less than 1:1, the structures are not regular at all (Figure S3D–I). It is worth mentioning that when the weight ratio of PS/SBS is 5:1, there is some parts of the holes are “missing” (Figure 4D). As shown in Figure 5, the average pore diameter and pore pitch increase with the adding SBS in two intervals, 1:0 to 8:1 and 5:1 to 3:1; but the pore size of later interval is less than the former's.

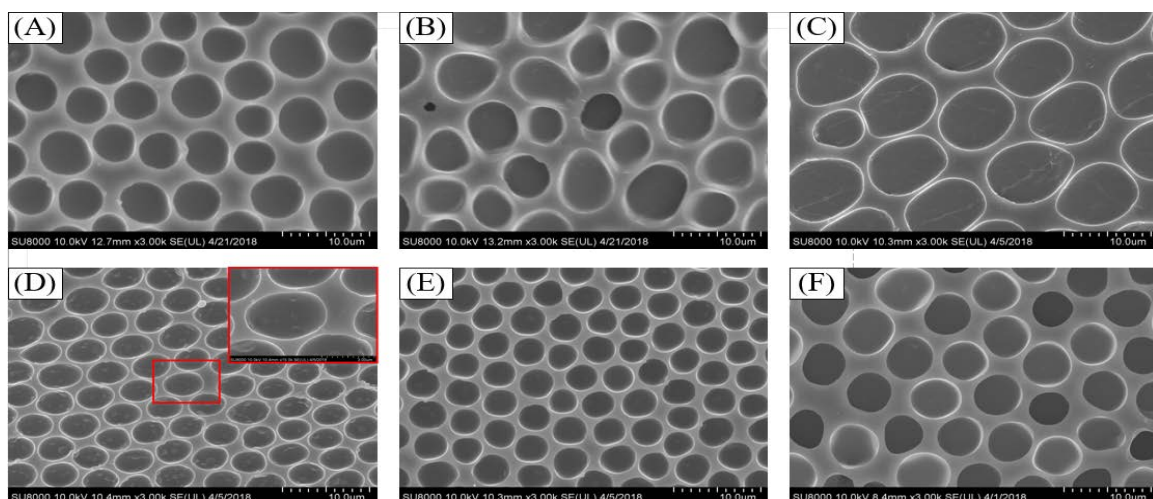


Figure 4. SEM images of PS/SBS porous films formed at different weight ratios of PS/SBS. (A) 1:0, (B) 10:1, (C) 8:1, (D) 5:1, (E) 4:1, (F) 3:1. Other factors: concentration of 50 g/L, the volume ratio of water/ethanol 3:1.

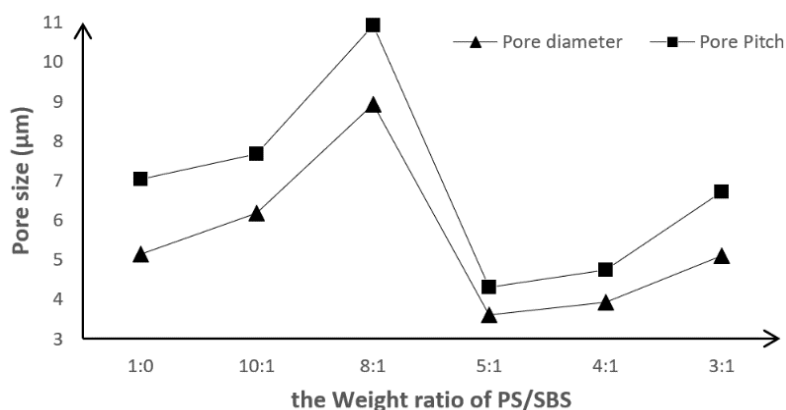


Figure 5. Plots of pore size versus the weight ratio of PS/SBS.

In this self-assembly system, the main force is the repulsion between PS block and PS phases of the SBS. As mentioned before, there exist some wrinkles due to the stresses released by the repulsion. A little SBS would disturb the balance of original system (pure PS solution), since the introduction of the soft PB phases or the PB phases is too little to offset the stresses produced by PS. When SBS is at a certain amount, the PB phases could offset the stresses for its soft property, and the structure is well-ordered. The PB block is likely to be “crushed” by the repulsion forces when the weight ratio of PS/SBS is lower 2:1 (which means the PB phases may take the majority of the blended polymer solution and the polymer is soft in the whole, and cannot resist the repulsive forces), so the structure is disordered. When the polymer is pure SBS, the repulsion produced is only from PS phase.

3.4. Influence of the Concentration

The concentration of the spreading solution can strongly influence the morphologies of the films' surface features. The concentration's influence on the porous films formation was investigated by changing the concentration of PS/SBS chloroform solution, which was from 10 g/L to 100 g/L. The weight ratio of PS/SBS was 3:1 and so did the volume ratio of the water/ethanol. As shown in Figure 6, the structure of the films is well-ordered when the concentration of solution is lower than 60 g/L, after that, the structure is becoming more and more disorder with the increase of the concentration, which indicates that concentration of the solutions influences the film's formation greatly. The average pore diameter and pore pitch show a general ascending trend which is from 2.73 μm to 7.26 μm for pore diameter and 4.29 μm to 8.26 μm for pore pitch when the concentration is lower than 100 g/L (the pore size decreases sharply) and with the fluctuate at 40 g/L and 60 g/L (Figure 7). However, it is noteworthy that there is no film formation when the concentration of the solution is lower than 30 g/L.

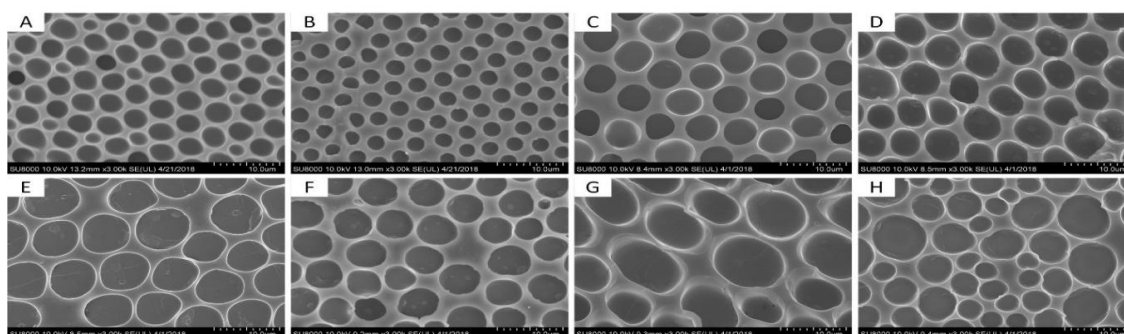


Figure 6. SEM images of PS/SBS porous films formed at different concentration. (A) 30 g/L, (B) 40 g/L, (C) 50 g/L, (D) 60 g/L, (E) 70 g/L, (F) 80 g/L, (G) 90 g/L (H) 100 g/L. Other factors: the weight ratio of PS/SBS 3:1, the volume ratio of water/ethanol 3:1.

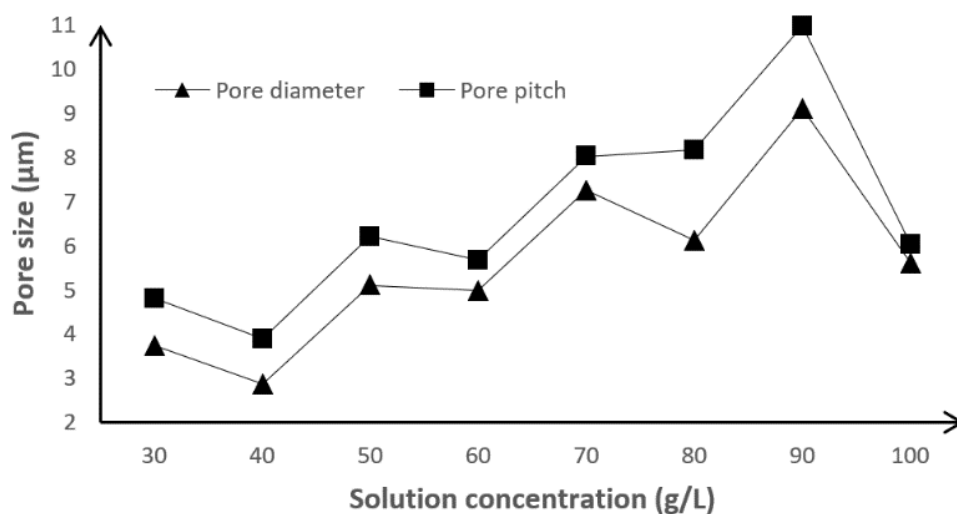


Figure 7. Plots of pore size versus solution concentration.

The observed differences in chain conformations which were formed within aggregates from different spreading concentrations can be explained by increased entanglements between PS blocks in more concentrated spreading solutions. As mentioned before, in the blended system, a certain amount of SBS can assist in the formation of the well-ordered structure, but when the SBS represents the majority, it has an opposite function. At a certain weight ratio of PS/SBS, the higher concentration of the spreading solutions means more PS chain entanglement with each other, and the polymer chain dynamics will be slower, so the less energetically favorable aggregate conformations are ultimately trapped by solvent removal. When the solution is at lower concentration, the PS chain has vitality to interact with each other and can form the well-ordered structure. When the surface tension of the solution decreases with the concentration's decrease, if the concentration of the solution is too low, the surface tension of the solution become lower and is unable to maintain a complete dip in a specific area, but it spread on the mixed liquid and formed small dots and chains when dipping the solution onto the surface of the mixed liquid.

3.5. Self-Cleaning Test

As mentioned before, the size of the films is around 1 cm^2 , and by carefully drop the polymer solution into the air-liquid interface continually and at the same place, films with a larger area can be obtained. Thereafter, we use glass as the substrate to hold the films. The films were fabricated at the concentration of solution is 40 g/L, the volume ratios of water/ethanol is 5:1, the weight ratio of PS/SBS is 3:1. According to capillary rise method, the surface tensions of water/ethanol solution and PS/SBS in chloroform were measured as 34.69 and 31.76 mN/m, respectively. The films were placed for 6 h in order to dry the films before putting in a lubricant for 1 h. Then we take the films out and put them vertically for 30 min to shed the extra oil.

The glass surfaces with and without the lubricant were fixed at a tilting angle 5° , then dipped in 0.5 mL of different pollutants (ink, blood). As can be seen from Figure 8C,D, after different times from the beginning pollutants were trapped in the dry films but moved to the bottom of the surface of the films; pollutants (hollow glass beads) were easily washed away by water on the surface of the films as shown in Figure 8E, which implies that the films have an excellent self-cleaning function which could be used in the areas such as endoscopes.

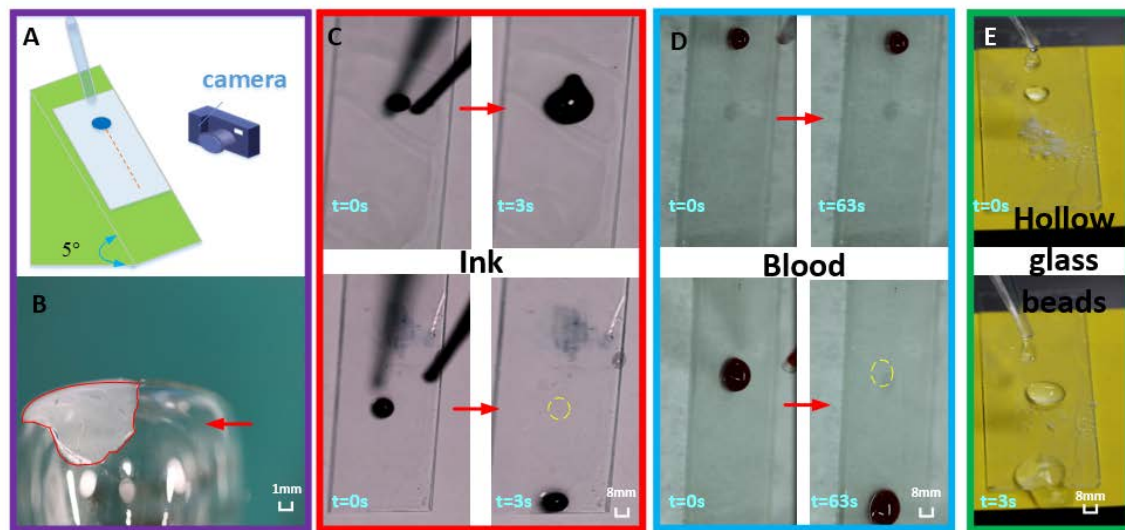


Figure 8. The images of porous films' self-cleaning functions for different pollutants. (A): test diagram. (B): the films can be applied on curved surface. (C): Ink, (D): Blood: the upper is dry and the lower is dealt with lubricant. (E): Water can easily wash away pollutants on the surface with dealt films.

Without treatment with lubricant, pollutants could enter the microstructure of the film surface. In this experiment, they could enter the pore structure of the film to cause the “pinning” phenomenon, that means the pollutants were “fixed” on the film, and the pollutants could not fall off the substrate easily. Due to the existence of the microstructure on the surface of the object, its roughness increased and the pollutants on it found it difficult to fall off. On the surface of the film treated with lubricant the latter occupied the position of the air in the pores, so the system changed from a solid-liquid-gas three-phase to a solid-liquid-liquid state and the liquid-liquid friction force is less than the friction force between liquid and gas, so pollutants could fall off from the super-slippy surface.

In order to compare the effects of film structure and lubricants on self-cleaning properties, four types of surfaces with differently processed were immersed in a beaker containing ink for about 3 s, respectively and then were taken out. Fierce contrast can be observed from Figure 9 that the composite surface of the film dealt with the lubricant shows marvelous self-cleaning ability.

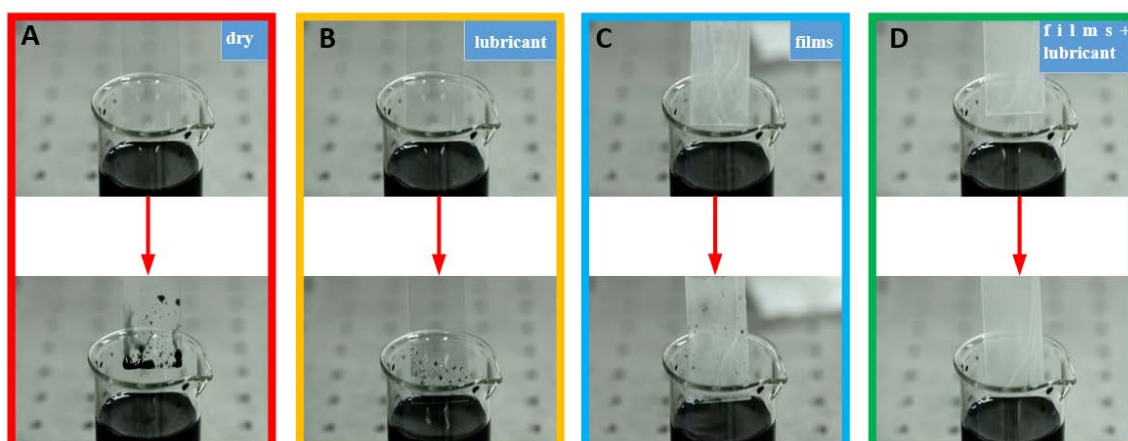


Figure 9. The images of comparison of self-cleaning functions. ((A): dry glass slide. (B): glass slide with lubricant. (C): the glass slide with films. (D): the glass slide with films dealt with lubricant).

The durability of self-cleaning function of the porous films was investigated by contrasting the sliding speed of the ink droplet on surfaces between wet porous film and wet flat film and the results were shown in Figure 10. As illustrated in Figure 10A, an ink droplet on the porous film surface slides

faster than that on flat film surface which verified the analysis above that the micropores on the surface are beneficial to enhance the slippery performance. Even though the surface with a flat film could also maintain good lubricity in previous experiments, however, as the number of experiments increased, the lubricating fluid was also consumed by the droplets. Therefore, after several experiments, it was difficult to slide down the inclined surface and the self-cleaning performance also weakened notably, as shown in Figure 10B. It can be proved that the structure of the porous film can trap the lubricating fluid compared with the structure of the flat film, and the lubricating durability is better and then the self-cleaning performance is also maintained.

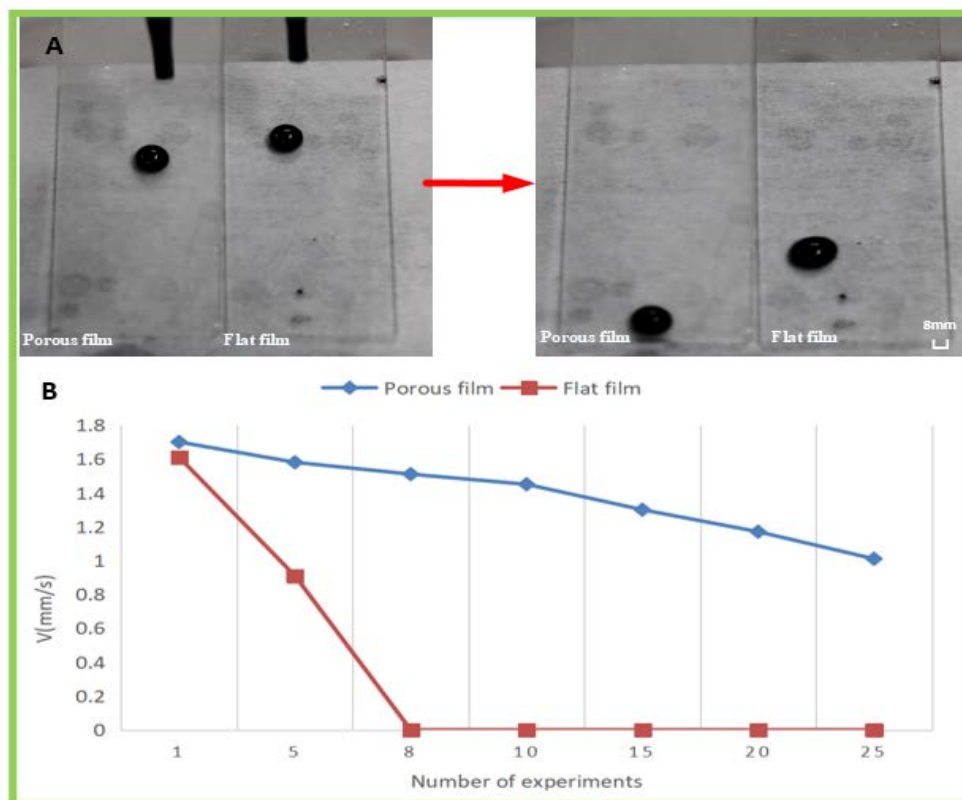


Figure 10. Comparison of self-cleaning performance between porous film and flat film ((A): Experimental picture; (B): Slip speed comparison curve of two films).

4. Conclusions

A new method to fabricate well-ordered PS/SBS porous films with different pore sizes by dipping the PS/SBS solutions onto the surface of a mixed water/ethanol liquid phase has been developed. The optimum volume ratios of water/ethanol are 3:1 to 6:1, and the concentration of PS/SBS chloroform solutions is lower than 60 g/L but greater than 20 g/L. The pattern regularity of the porous films increases with lower solution concentration. The weight ratio of PS/SBS makes a great contribution to the well-ordered microstructure formation of the films. The weight ratio of PS/SBS between 3 and 4 is the best choice according to the experimental results. However, no well-ordered porous films are obtained when the weight ratio of PS/SBS is less than 1:4 and no films are obtained at all when the volume ratio of water/ethanol is lower than 2:1. This facile strategy to fabricate well-ordered porous films may provide an ideal route to make microstructures in sensors, fuel cells and micro-devices design more applicable.

After the prepared film is treated with lubricant, its self-cleaning performance is greatly improved. On the film that is not treated with lubricant, pollutant retention has a strong dependence on the surface of the film. After being treated with lubricant, it has good self-cleaning performance. When the

glass surface is fixed at a tilting angle at 5°, the tested pollutants (i.e., ink, blood and hollow glass beads) can easily fall off the film surface. The film assembled on the liquid surface can be well attached to a free-form surface, which is expected to be applicable to anti-fouling treatment of free-form surfaces such as endoscopes that are prone to fluid stickiness.

Supplementary Materials: The following are available online at <http://www.mdpi.com/2079-6412/10/11/1133/s1>, Figure S1: Image of PS/SBS porous films with large ordered structure, Figure S2: SEM images of PS/SBS porous films with the “peristome” at volume ratio of water/ethanol 2:1, Figure S3: SEM images of PS/SBS porous films formed at different weight ratios of PS/SBS.

Author Contributions: Y.L., H.C. and D.Z. conceived and designed the experiments; Y.L., J.D. and X.Z. performed the experiments; Y.L., J.D. and Y.W. analyzed the data; Y.L., H.C. and D.Z. discussed the results. Y.L. and J.D. wrote the initial manuscript which was approved by all the authors. All authors have read and agreed to the published version of the manuscript.

Funding: This research was funded by National Science Fund for Distinguished Young Scholars grant number [51725501].

Conflicts of Interest: The authors declare no conflict of interest.

References

1. Wijnhoven, J.E.; Vos, W.L. Preparation of Photonic Crystals Made of Air Spheres in Titania. *Science* **1998**, *281*, 802–804. [[CrossRef](#)] [[PubMed](#)]
2. Lewandowski, K.; Murer, P.; Frantisek, S.; Jean, M. The Design of Chiral Separation Media Using Monodisperse Functionalized Macroporous Beads: Effects of Polymer Matrix, Tether, and Linkage Chemistry. *Anal. Chem.* **1998**, *70*, 1629–1638. [[CrossRef](#)] [[PubMed](#)]
3. Yan, F.; Goedel, W.A. A Simple and Effective Method for the Preparation of Porous Membranes with Three-Dimensionally Arranged Pores. *Adv. Mater.* **2004**, *16*, 911–915. [[CrossRef](#)]
4. Shastri, V.P.; Martin, I.; Langer, R. Macroporous polymer foams by hydrocarbon templating. *Proc. Natl. Acad. Sci. USA* **2000**, *97*, 1970–1975. [[CrossRef](#)] [[PubMed](#)]
5. Xuan, S.; Zhang, Z.; Chen, Z.; Chen, Y. Porous Structure Fabrication Using a Stereolithography-Based Sugar Foaming Method. *J. Manuf. Sci. Eng.* **2017**, *139*, 031015.
6. Yabu, H.; Shimomura, M. Mesoscale pincushions, microrings, and microdots prepared by heating and peeling of self-organized honeycomb-patterned films deposited on a solid substrate. *Langmuir ACS J. Surf. Colloids* **2006**, *22*, 4992–4997. [[CrossRef](#)] [[PubMed](#)]
7. Alexandra, M.; Marta, F.; Juan, R. Towards hierarchically ordered functional porous polymeric surfaces prepared by the breath figures approach. *Prog. Polym. Sci.* **2014**, *39*, 510–554.
8. Alexander, B.; Yao, L.; Kristen, C.; Reina, H. Hierarchical nanoparticle assemblies formed by decorating breath figures. *Nat. Mater.* **2004**, *3*, 302–306.
9. Hiroshi, Y. Fabrication of honeycomb films by the breath figure technique and their applications. *Sci. Technol. Adv. Mater.* **2018**, *19*, 802–822.
10. Rahmawan, Y.; Xu, L.B.; Yang, S. Self-assembly of nanostructures towards transparent, superhydrophobic surfaces. *J. Mater. Chem. A* **2013**, *1*, 2955–2969. [[CrossRef](#)]
11. Yabu, H.; Shimomura, M. Single-Step Fabrication of Transparent Superhydrophobic Porous Polymer Films. *Chem. Mater.* **2005**, *17*, 5231–5234. [[CrossRef](#)]
12. Liu, Y.; Xu, Q.F.; Lyons, A. Durable, optically transparent, superhydrophobic polymer films. *Appl. Surf. Sci.* **2019**, *470*, 187–195. [[CrossRef](#)]
13. Chang, K.C.; Chen, Y.K.; Chen, H. Fabrication of superhydrophobic silica-based surfaces with high transmittance by using polypropylene and tetraethoxysilane precursors. *J. Appl. Polym. Sci.* **2008**, *107*, 1530–1538. [[CrossRef](#)]
14. Maedeh, R.; Mohammad, R.V.; Asghar, K. Preparation of silane-functionalized silica films via two-step dip coating sol-gel and evaluation of their superhydrophobic properties. *Appl. Surf. Sci.* **2014**, *317*, 147–153.
15. Imhof, A.; Pine, D.J. Ordered macroporous materials by emulsion templating. *Nature* **1997**, *389*, 948–951. [[CrossRef](#)]
16. Xu, L.; Karunakaran, R.G.; Guo, J.; Yang, S. Transparent, superhydrophobic surfaces from one-step spin coating of hydrophobic nanoparticles. *ACS Appl. Mater. Interfaces* **2012**, *4*, 1118–1125. [[CrossRef](#)]

17. Li, Y.; Men, X.; Zhu, X.; Ge, B.; Chu, F.; Zhang, Z. One-step spraying to fabricate nonfluorinated superhydrophobic coatings with high transparency. *J. Mater. Sci.* **2016**, *51*, 2411–2419. [[CrossRef](#)]
18. Kim, F.; Kwan, S.; Akana, J.; Yang, P. Langmuir–Blodgett Nanorod Assembly. *J. Am. Chem. Soc.* **2001**, *123*, 4360–4361. [[CrossRef](#)]
19. Vogel, N.; Goerres, S.; Landfester, K.; Weiss, C. A Convenient Method to Produce Close- and Non-close-Packed Monolayers using Direct Assembly at the Air–Water Interface and Subsequent Plasma-Induced Size Reduction. *Macromol. Chem. Phys.* **2011**, *212*, 1719–1734. [[CrossRef](#)]
20. Oh, S.; Yang, M.; Bouffard, J.; Hong, S.; Park, S. Air-Liquid Interfacial Self-Assembly of Non-Amphiphilic Poly(3-hexylthiophene) Homopolymers. *ACS Appl. Mater. Interfaces* **2017**, *9*, 12865–12871. [[CrossRef](#)]
21. Chokprasombat, K.; Sirisathitkul, C.; Ratphonsan, P. Liquid–air interface self-assembly: A facile method to fabricate long-range nanoparticle monolayers. *Surf. Sci.* **2014**, *621*, 162–167. [[CrossRef](#)]
22. Wang, L.; Sun, Y.; Che, G.; Li, Z. Self-assembled silver nanoparticle films at an air–liquid interface and their applications in SERS and electrochemistry. *Appl. Surf. Sci.* **2011**, *257*, 7150–7155. [[CrossRef](#)]
23. Kadota, S.; Aoki, K.; Nagano, S.; Seki, T. Photocontrolled microphase separation of block copolymers in two dimensions. *J. Am. Chem. Soc.* **2005**, *127*, 8266–8267. [[CrossRef](#)] [[PubMed](#)]
24. Zhao, L.; Feng, C.W.; Pang, X.C.; Jung, J.; Mihaela, C.; Prakash, S.; Han, R.; Ning, F.; Lin, Z. Self-assembly of a conjugated triblock copolymer at the air–water interface. *Soft Matter* **2013**, *9*, 8050–8056. [[CrossRef](#)]
25. Zhang, X.M.; Li, L.; Zhang, Y. Study on the Surface Structure and Properties of PDMS/PMMA Antifouling Coatings. *Phys. Procedia* **2013**, *50*, 328–336. [[CrossRef](#)]
26. Cativo, M.; Helen, M.; Kim, D.K.; Riggelman, R.A.; Yager, K.; Nonnenmann, S. Air-liquid interfacial self-assembly of conjugated block copolymers into ordered nanowire arrays. *ACS Nano* **2014**, *8*, 12755–12762. [[CrossRef](#)]
27. Baker, S.M.; Leach, K.A.; Devereaux, C.E.; Gragson, D.E. Controlled Patterning of Diblock Copolymers by Monolayer Langmuir–Blodgett Deposition. *Macromolecules* **2000**, *33*, 5432–5436. [[CrossRef](#)]
28. Jin, Y.P.; Advincula, R.C. Nanostructuring polymers, colloids, and nanomaterials at the air–water interface through Langmuir and Langmuir–Blodgett techniques. *Soft Matter* **2011**, *7*, 9829–9843.
29. Adhikari, R.; Huy, T.A.; Buschnakowski, M.; Michler, G.; Knoll, K. Asymmetric PS-block-(PS-co-PB)-block-PS block copolymers: Morphology formation and deformation behavior. *New J. Phys.* **2004**, *6*, 28–47. [[CrossRef](#)]
30. Vilaplana, F.; Osorio-Galindo, M.; Iborra-Clar, A.; Alcaina-Miranda, M.; Ribes-Greus, A. Swelling behavior of PDMS–PMHS pervaporation membranes in ethyl acetate–water mixtures. *J. Appl. Polym. Sci.* **2004**, *93*, 1384–1393. [[CrossRef](#)]
31. Cheyne, R.B.; Moffitt, M.G. Novel two-dimensional “ring and chain” morphologies in Langmuir–Blodgett monolayers of PS-b-PEO block copolymers: Effect of spreading solution concentration on self-assembly at the air–water interface. *Langmuir* **2005**, *21*, 5453–5460. [[CrossRef](#)] [[PubMed](#)]
32. And, C.A.D.; Baker, S.M. Surface Features in Langmuir–Blodgett Monolayers of Predominantly Hydrophobic Poly(styrene)–Poly(ethylene oxide) Diblock Copolymer. *Macromolecules* **2002**, *35*, 1921–1927.

Publisher’s Note: MDPI stays neutral with regard to jurisdictional claims in published maps and institutional affiliations.



© 2020 by the authors. Licensee MDPI, Basel, Switzerland. This article is an open access article distributed under the terms and conditions of the Creative Commons Attribution (CC BY) license (<http://creativecommons.org/licenses/by/4.0/>).